An Application of K-ε Turbulence Model for Predicting Effect of a Rectanguler Obstacle with Heat Flux in a Solt-Ventilated Enclosure on Air Flow

Choi, Hong Lim* · Kim, Hyeon Tae · Kim, Woo Joong*****

**Associate Professor, Dept. of Agric. Engr., Gyeongsang Natioal University, Jinju, Republic of Korea, 660-701*

***Research Assistant, Dept. of Agric. Engr. Gyeongsang Natioal University, Jinju, Republic of Korea, 660-701*

****Lecturer, Dept. of Agricultural Civil Engineering, Chinju Polytechnic College, Jinju, Republic of Korea 660- 290*

Abstract□A modification of the TEACH-like computer program based on the k-ε turbulence transport was applied for predicting air mixing patterns and temperature distributions in a rectangular, slot-ventilated enclosure having obstructions ; a rectangular obstacle with heat flux, solid walls separates the passage and the pig pens, and purlins beneath the ceiling. Air flow patterns were calculated for the cases with and without the purlin, extending 300mm beneath the ceiling. Comparisons of prediction data of Randall & Battams(1976) showed air flow pattern predicted well for the case without the purlin. Heat was accumulated at the corner of the left side of the solid wall and the right-upper region of the simulated pigs. However the air distribution pattern was completely different from data for the case with the purlin. The deviation from the observation may be attributed to the difference of the geometric configuation. Exploring the cause of the deviation should be conducted in a further study. Temperature stratification was also observed due to incomplete mixing. The obstruction in the route of the inlet air jet at inlet should be avoided since most of kinetic energy dissipates at the abstacle duet to impingement.

Keywords□K-ε turbulence transport, obstruction, heat flux, air flow pattern, temperature

I. Introduction

Rapid rise of the value of land and labor leads livestock bulidings in Korea to be larger, denser, more confined, and automatized. It is known that improper environment lowers production and reproduction of animals in a confined livestock building. (Hellickson & Walker, 1983 ; Choi, 1989). To provide optimum environment for animals and workers, it is needed to control environmental pa-

rameters influencing indoor air quality.

Generally, temperature, humidity, and contaminants (dust and harmful gases) are known as major environmental parameters to be controlled. Barber(1981) concluded that mechanical ventilation is a practically acceptable medium to dilute contaminants in a confined livestock building. A typical ventilation graph for determining the ventilation rate to control temperature and humidity in a livestock building was introduced in Hong-lim Choi (1988) and Hellickson & Walker(1983). A new conceptual ventilation graph including additional parameters for determining the ventilation rate was suggested by Choi(1991), Albright(1984). ASHRAE(1989), and Hellickson & Walker(1983). However, these works have been basically done for determination of the ventilation rate quantitatively.

It often happens that incoming air is exhausted to outlet without mixing with existing indoor air (bypassing or short-circuiting) or air speed reaches almost zero in some regions(dead zone or stagnant zone) so that ventilation air flow does not dilute effectively contaminants in a building. Determining the ventilation rate based on the ventilation graphs is necessary but not sufficient. Therefore a quantitative study should go along with a qualitative study to confirm the effectiveness of the ventilation system for a livestock building (Albright, 1984). A qualitative study includes predicting scalars (temperature, humidity and contaminants) distributions in a ventilated building, of which motion is determined by air flow. Therefore, it is important to explore air flow patterns and temperature distribution in a livestock building, which provides basic information for optimum design of the ventilation system.

Choi et al.(1988, 1900) studied the air flow patterns in a slat-ventilated enclosure with and without obstruction.

The work presented in this article was to investigate the effects of buoyancy force to air flow, created by the temperature difference between the temperature of entering air jet and that of the simulated pigs, and the effects of obstruction, purlin in the route of the inlet air jet, using a modified version of the TEACH-like computer program for steady-state, two dimensional, non-isothermal, and recirculating flow in a ventilated livestock building.

II. Literature Review

Fairbanks(1929, 1932) made a significant contribution to the ventilation system design of a modern livestock building although his work was not based on solid theory or extensive experiments. He introduced the design concept of slotted inlet system and the possibility of using electric fans to exhaust air from the building. He also cirticized the heavy dependence on the number of air changes, saying that the number is not a sufficient indicator of adequate ventilation based on his researches. This suggested a quantitative study was not sufficient due to the possibility of the deviation from complete mixing.

Pattie & Milne(1966) conducted a small scale model study for two dimensional, isothermal flow in order to investigate the air flow patterns and air velocities in broiler houses using several different types of inlet configuations. Their data indicated that air flow patterns are governed by the configuration of the air inlet and flow patterns air independent of the Reynolds number if the Reynolds number is greater than a threshold value. Their observation of the importance of air

viscosity and the analogical inference of the qualitative similarity of air flow patterns between the model and the prototype with different inlet configurations should be further discussed to validate. The work displayed the experimented flow patterns with several different types of inlet configurations.

Similar work with Pattie and Milne (1966)'s was conducted by Timmons(1984) to reaffirm the validity of using a small scale model to predict air flow patterns in a ventilated space of a full-scale structure. The similarity analysis was applied based on the selection of pertinent variables governing the pheonomenon and subsequent organization of appropriate dimensionless combinations of these variables. The accuracy of the prediction of air movement depends on geometric, kinematic. and dynamic similarities. The characteristic of steady, incompressible, isothermal flow in a ventilated space was written as a function a Reynolds number and length scale :

$$V_D[x, y] = f[R, L_D] \quad (1)$$

Where, V_D : dimensionless velocity in 2-D flow
R : Reynolds number
L_D : dimensionless kinematic length

All the relationship of geometric scaling are defined as :

$$l_m = l_p/n \quad (2)$$

Where, l_m : length of the model
l_p : length of the prototype structure
n : length scale

Small scale models were made and experimented based on Eqs.(1) and (2) to satisfy the geometric and knematic similarities. Timmons confirmed the observation of Pattie and Milne (1966) that air flow patterns are independent of the Reynolds number above a threshold Reynold number. He observed the thershold Reynolds number, R, increases with physical size of the small scale models and the location of the outlet affected the size of the secondary circulation area. It is generally understood that the location of the outlet does not influence air movement since the state of the downstream flow is determined solely by the state of upstream flow. The accuracy of velocity predictions based on small scale models seems reasonable.

However, improvements can be made by examining the governing equations using experimental observation. For example, he did not involve a pressure term in Eq.(1), assuming that the pressure term can be neglected at high Reynolds numbers. Tennekes and Lumley (1972), however, showed by approximation of the V-momentum equation through the order of magnitude analysis that the square of the fluctuating lateral velocity is balanced solely with pressure gradient in the horizontal direction, although the pressure gradient of outside turbulent flow was imposed to zero. Thus involvement of the pressure term in the analysis of Eq. (1) may give more accurate results in velocity distributions.

A more realistic prototype ventilation study than Pattie and Milne (1966) was conducted by Turnbull and Coates (1971) to evalulate summer and winter ventilation performance of a new, triple-deck, cage rearing facility for replacement pullets at a modern commercial scale poultry house. This study provideds useful information about air flow patterns and temperature distributions under field conditions, and introduced the concept of ventilation system modification, by combining two inlet systems for best effectiveness of the ventilation system. Their evaluation of summer and winter

ventilation performances based on temperature distributions over space may be generally acceptable. However, if ventilation performance is evaluated in terms of overall air quality, involving additional parameters like concentration of harmful gases and/or dust, it may produce a different outcome. This is the case whether or not ventilation performance can be evaluated by temperature distributions alone or by some new method.

Carpenter et al. (1972) visualized air flow patterns using illuminated liquid-film bubbles with photographic imaging in a prototype livestock building. They reported the use of the bubble visualization is a valid and useful technique to investigate air movement in a prototype experimental space. However, since the adjustment of the parameters structure is both difficult and expensive for a full-scale structure, it is not readily adaptable for prediction of air movement in a livestock buiiding.

Randall (1975) conducted a similar but more complete prototype experimental study than Carpenter et al. (1972). He used a full scale of a typical livestock building with transparent gables to visualize the air flow patterns for combinations of penning arrangement and ventilation rate under isothermal and non-isothermal conditions. The effect of physical obstrutions and temperature gradients on air flow patterns were stressed and carfully studied. He observed that physical obstructions modify air flow patterns more than any other parameters. He also observed that at a lower ventilation rate air flow movement becomes less stable and more senstive to the temperature gradient at a lower ventilation rate. Thus air flow patterns were shown to change substantially with relative small increment of ambient temprature, resulting in the creation of stagnant regions. He confirmed through his experiments that the air inlet system mainly controls air flow patterns in a ventilated space. Although he did not provide by any theoretical developments on air movement. Randall provided and insight on air flow patterns for the full scale livestock building. If the theoretical simulation can be achieved. Randall's work will be a good source of date for comparison.

A series of prototype scale studies in England has been continued by Boon (1978) to investigate the air flow patterns and temperature distributions in a livestock building. He performed experiments similar to Randall's (1975) but he used different layouts from Randall's claiming that Randall's combinations of penning arrangements and ventilation system were impractical. Boon observed air flow patterns with combinations of penning arrangements, ventilation systems, and temperature regimes. The building section was surrrounded above and on two sides by an outer shell to eliminate external temperature variations. Scuh a structural disign for experiments made it possible to obtain accuarte date for the temperature effect on air flow patterns and temperature distributions. He observed that air flow patterns were stable when the temperature of inlet air jet T_{in}〉15℃, or when T_{in}〈11℃. Air flow patterns were unstable in the temperature range of 11℃〈Tin〈15℃ for a building section temperature of 18℃. He reported for high inlet jet temperature, that a more uniform distribution of temperature occured when the jet was directed downward along the wall, rather than directed horizontally, which may result in short-circuiting of the inlet air flow. At the lower temperature of the air inlet jet, temperature distributions were not much different from one another, irrespective of whether or not the air jet was directed or down by inlet baffles.

No paper reviewed so far have employed fluid dynamic theory in investigating air flow behavior in a ventilated space. Specifically, the Navier-Stokes equations are known to properly discribe the fluid motion in a ventilated space. Other researchers have attempted to simulate air flow patterns or velocity distributions by using the modified Navier-Stokes equations with some other auxilliary transport equations.

Timmons (1979) formulated the modified inviscid Navier-Stokes equation (vorticity equation) and validated the results with scale study. To simulate overall air flow patterns and air velocity distribution for a certain flow geometry, he started with the assumption that the main source of vorticity production occurs at the inlet, and ignored other possible vorticity productions. His basic premise was that vorticity calculated by knowing the velocity profile at the inlet, should transport and redistribute over the space.

The vorticity transport equation reads :

$$\frac{D\omega}{Dt} = \nu\nabla^2\omega \qquad (3)$$

where

$D/Dt = \partial/\partial t + \partial/\partial x + \partial/\partial y$ (material derivative)

$\omega = \partial V/\partial x - \partial U/\partial x$ (vorticity)

$\nabla = \partial^2/\partial x^2 + \partial^2/\partial y^2$ (Laplace operator)

Eq.(3) was further simplified by the assumption of inviscidness. Thus it reduces to :

$$\frac{D\omega}{Dt} = 0 \qquad (4)$$

Eq.(4) implies that vorticity is conserved throughout a ventilated space for steady state flow conditions. In other words, vorticity is constant along streamlines in physical sense.

$$\omega = f[\psi] \qquad (5)$$

The essence of the model is that it established the relations of the general vorticity equation in terms of stream functions with the help of Eq.(5).

$$\nabla^2\psi = -\omega = F[\psi] \qquad (6)$$

The distribution of stream function over space can be determined by knowing vorticity distribution through Eq.(6). Air flow patterns predicted by the inviscid vorticity model were agreeable with those observed experimentally. However, it is not difficult to see limitations of the model. The assumption of inviscidness results inexceedingly high velocities near walls.

The major attractive feature of the stream function-vorticity(ψ-ω) method is to eliminate the need to handle the pressure term from the momentum equations which is difficult to determine. However, there are serious disadvantages which can not compensate the advantages of the application of this method to flow motion. The value of vorticity at walls is difficult to specify and is often the cause of an inability to attain a converged solution. Secondly, the pressure frequently is an important desired result or even an intermediate outcome required for the calculation of density and other fluid properties. Thirdly, a major shortcoming of the method is that it cannot be extended to three dimensional situation, for which a stream funtion does not exist (Patanker, 1980). Since most practical engineering applications are three dimensional problem, and the stream function-vorticity method is intrinsically restricted to two dimensions, this is a serious limitation. As mentioned earlier. Timmons(1984) work should share these shortcomings of the method which he used for the prediction of flow motion.

Application of ventilation to fields other than agricultural engineering(i.e. ventilation of livestock buildings, greenhouses, or ware houses) is quite

common. A review of these works has been eliminated in this study in order to concentrate on the livestock buildings. The fundamentals of ventilation analysis are the same for agricultural structures and general structures. The only difference lies in the type of objects in a structure. Animals or crops are the primary objects in agricultural structures whereas people for general structures.

III. Mathermatical Model

1. Statistical Approach

Air motion in a livestock building is bascially turbulent flow, which is governed by the law of mass momentum and energy conservation. Navier-Stockes equation cannot be applicable to turbulent flow due to its nature. A statistial approach is taken and as suggested by Osborne Reynolds that the instantaneous values of the velocity, U_i, and the scalar quantity, Φ, are separated into mean and fluctuating quantities (Rodi, 1980) :

$$U_i = \overline{U}_i + u_i, \quad \Phi = \overline{\Phi} + \phi \tag{7}$$

Introducing Eq.(7) to the continuity equation, momentum and scalar transport equation and subsequent averaging yields the following equations:

1) Continuity :

$$\frac{\partial \rho}{\partial t} + \frac{\partial}{\partial x_i}(\rho U_i) = 0 \tag{8}$$

2) Momentum Equation :

$$\frac{\partial}{\partial t}(\rho U_i) + U_j \frac{\partial}{\partial x_j}(\rho U_i) = -\frac{\partial P}{\partial x_i} + \frac{\partial}{\partial x_j}$$

$$(\mu \frac{\partial U}{\partial x_j} - \rho \langle u_i u_j \rangle) + g_i(\frac{\rho - \rho_r}{\rho_r}) \tag{9}$$

3) Scalar Equation :

$$\frac{\partial}{\partial t}(\rho \Phi) + U_i \frac{\partial}{\partial x_i}(\rho \Phi) = \frac{\partial}{\partial x_i}(\Gamma \frac{\partial \Phi}{\partial x_i} - \langle u_j \phi \rangle)$$

$$+ S_h \tag{10}$$

The averaging process introduces unknown correlations between fluctuating velocities, $\langle u_i u_j \rangle$, in Eq.(9) and scalar fluctuations, $\langle u_i \phi \rangle$, in Eq.(10). Physically, these correlations, multiplied by the density, ρ, represent the transport of momentum and scalar due to turbulent motion. The determination of these correlations is the main problem in calculating turbulent flows. In practice, a turbulent model can be in introduced which approximates the correlations of a certain order in terms of lower and/or mean flow quantities.

2. Turbulence Model(two-equation models : k-ε Model)

The oldest proposal for modeling the turbulent or Reynolds stress, $-\rho \langle u_i u_j \rangle$ turned out to become a significant part of most turbulence models of practical use today. Boussinesq's eddy-viscosity concept which assumes that in analogy to the viscous stresses in laminar flows, the turbulent stresses are proportional to the mean-velocity gradients. For general flow situations, this concept may be expressed as :

$$-\rho \langle u_i u_j \rangle = -\mu_t (\frac{\partial U_i}{\partial x_j} + \frac{\partial U_i}{\partial x_i}) - 2/3\, \rho\, k\, \delta_{ij} \tag{11}$$

Turbulent viscosity(μ_t), in contrast to the molecular viscosity(μ), is not a fluid property but depends strongly on the state of turbulence. μ_t may vary significantly from one point in the flow to another and also from flow to flow. The introduction of Eq.(11) alone does therefore not constitute a turbulence model but only provides the framework constructing such a model. The main problem is now shifted to determining the distribution of μ_t.

Turbulence is assumed to be characterized by the turbulent kinetic energy, k, and its dissipation rate, ε, known as the two-equation turbulence model. Turbulent viscosity is determined by local va-

lues of k and ε.

$$\mu_t = C\mu\,\rho\,\frac{k^2}{\varepsilon} \tag{12}$$

3. Governing Equations

The governing differential equations of turbulent flow take the following forms for steady-state, two dimentisonal, non-isothermal mean flow. The equations are expressed in the Cartesian coordinate system having a horizontal direction, x, with its directional mean velocity, U, and a vertical direction, y, with its directional mean velocity, V.

1) Continuity :

$$\frac{\partial \rho}{\partial t} + \frac{\partial}{\partial x}(\rho U) + \frac{\partial}{\partial y}(\rho V) = 0 \tag{13}$$

2) U-Momentum Equation :

$$\frac{\partial}{\partial t}(\rho U) + \frac{\partial}{\partial x}(\rho U^2) + \frac{\partial}{\partial y}(\rho U V) = -\frac{\partial P}{\partial x} + \frac{\partial}{\partial x}(\mu_t \frac{\partial U}{\partial x}) + \frac{\partial}{\partial y}(\mu_t \frac{\partial V}{\partial x}) + S_u \tag{14}$$

Where, $S_u = \frac{\partial}{\partial x}(\mu_t \frac{\partial U}{\partial y}) + \frac{\partial}{\partial y}(\mu_t \frac{\partial V}{\partial x})$

3) V-Momentum Equation :

$$\frac{\partial}{\partial t}(\rho V) + \frac{\partial}{\partial x}(\rho U V) + \frac{\partial}{\partial y}(\rho V^2) = -\frac{\partial P}{\partial y} + \frac{\partial}{\partial x}(\mu_t \frac{\partial U}{\partial y}) + \frac{\partial}{\partial y}(\mu_t \frac{\partial V}{\partial y}) + \rho_r g\beta(T - T_r) + S_v \tag{15}$$

where, $S_v = \frac{\partial}{\partial x}(\mu_{eff} \frac{\partial V}{\partial x}) + \frac{\partial}{\partial y}(\mu_{eff} \frac{\partial V}{\partial y})$

4) Energy Transport Equation :

$$\frac{\partial}{\partial t}(\rho h) + \frac{\partial}{\partial x}(\rho U h) + \frac{\partial}{\partial y}(\rho V h) = \frac{\partial}{\partial x}(\gamma_{eff} \frac{\partial h}{\partial x}) + \frac{\partial}{\partial y}(\gamma_{eff} \frac{\partial h}{\partial y}) + S_h \tag{16}$$

where, S_h : source terms like heat flux

5) Turbulent kinetic energy equation (k-equation) :

$$\frac{\partial}{\partial t}(\rho k) + \frac{\partial}{\partial x}(\rho U k) + \frac{\partial}{\partial y}(\rho V k) = \frac{\partial}{\partial x}(\frac{\mu_{eff}}{\sigma_k} \frac{\partial k}{\partial x}) + \frac{\partial}{\partial y}(\frac{\mu_{eff}}{\sigma_k} \frac{\partial k}{\partial y}) + G - C_D \rho\varepsilon + - G_B \tag{17}$$

where, $G = \mu_t[\{2(\frac{\partial U}{\partial x})^2 + (\frac{\partial V}{\partial y})^2\} + (\frac{\partial U}{\partial y} + \frac{\partial V}{\partial x})^2]$

$G_B = \beta g(\frac{\mu t}{\sigma_t}) \frac{\partial \theta}{\partial y}$

$\theta = T - T_r$

6) Dissipation rate of Turbulent Kinetic Energy (ε-equation) :

$$\frac{\partial}{\partial t}(\rho \varepsilon) + \frac{\partial}{\partial x}(\rho U \varepsilon) + \frac{\partial}{\partial y}(\rho V \varepsilon) = \frac{\partial}{\partial x}(\frac{\mu_{eff}}{\sigma_e} \frac{\partial \varepsilon}{\partial x}) + \frac{\partial}{\partial y}(\frac{\mu_{eff}}{\sigma_e} \frac{\partial \varepsilon}{\partial y}) + \frac{\varepsilon}{k}(C_1 G - C_2 \rho \varepsilon) + C_3 \frac{\varepsilon}{k} G_B \tag{18}$$

Table 1. Value of constants in the turbulence model

C_μ	C_D	C_1	C_2	C_3	σ_k	σ_e
0.09	1.0	1.44	1.92	1.0	1.0	1.3

IV. Numerical Analysis

1. Formulation of Discretized Equations

Eq.(13)~(18) can be described by the differential equations of the form for single phase flow. $\phi = 1$ yields the continuity equation.

$$\frac{\partial}{\partial t}(\rho \phi) + \nabla(\rho \phi V) - \nabla(\Gamma_s \nabla \phi) = S_s \tag{19}$$

The values of the flow varibles at each cell and for each time-step are the sought-for outcome of the computation. Fig. 1(a) is the control voulme for scalar and (b) for velocities. The code uses the staggered-grid arrangement(Fig. 1(b)), in which the location of the velocity nodes is displa-

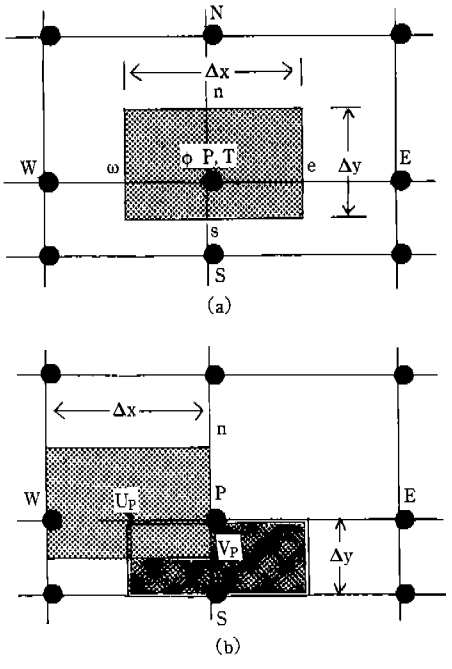

Fig. 1. Two dimensional calculation domain for (a) scalar (b) U-velocity(▒), V-velocity (▓) in cartesian coordinate

ced with respect to the location of the node used for other scalar variables, and located on the cell faces. The benefits of this arrangement are that each velocity component is driven by two adjacent pressures and the value of the velocity is avaiable, without interpolation, at the cell face, where it will be needed to compute the convection fluxes into cell.

The results of the intergration process can be grouped into an equation of the form :

$$a_P\phi_P = a_N\phi_N + a_S\phi_S + a_E\phi_E + a_W\phi_W + a_T\phi_T + b \quad (20)$$

where, $a_E = \rho A_E[-U_e] + D_E$

$a_T = (V_P/\Delta t)\,\rho_T$

$b = V_P\, C\phi_P\, V\phi_P$

Note that the diffusion contribution to the a's, for example $De = \frac{\Gamma_P + \Gamma_E}{2}\frac{A_e}{|PE|}$ is further multiplied by the factor $[1.0 - \zeta|F_e/D_e|]$ where F_e is the convection contribution through the cell face in the calculation domain, $F_e = \rho_P\phi_P\ A_E[U_e] - \rho_E\phi_E\ A_E[-U_E]$ for $\zeta = 0.0$, this yields the upwind scheme. For $\zeta = 0.5$, the hybrid scheme results. Note that F_E/D_E is a Pecklet number.

Eq.(20) can be rewritten for ϕ_P as :

$$\phi_P = \frac{a_E\phi_E + a_W\phi_W + a_N\phi_N + a_S\phi_S + a_T\phi_T + b}{a_E + a_W + a_N + a_S + a_T + a_P} \quad (21)$$

2. Definition of the Exchange Coefficient

The formulae used for the exchange coefficients are governed by the settings of the PIL variable PRL(ϕ) and PRT(ϕ), where ϕ denotes the dependent variable in question. These formulas involve the fluid density, the molecular and turbulent kinematic viscosities, denoted by μ_l and μ_t respectively, and the molecular and turbulent Prandtl numbers, denoted by σ_l and σ_t respectively.

The exchange coefficient in Eq. (22) may optionally be expressed in terms of the laminar and/or turbulent diffusivities, denoted by D_l and D_t respectively. The PIL variables PRL(ϕ) and PRT(ϕ) have the significance of a Prandtl number it they are given positive values, but negative values have the significance of diffusivity.

(i) if $Pr_t(\phi)>0 \,\&\, Pr_l(\phi)>0$: $\Gamma_{P,\phi} = (\mu_t/\sigma_{t,\phi} + \mu_l/\sigma_{l,\phi})$

(ii) if $Pr_t(\phi)<0 \,\&\, Pr_l(\phi)>0$: $\Gamma_{P,\phi} = (D_{t,\phi} + \mu_l/\sigma_{l,\phi})$

(iii) if $Pr_t(\phi)>0 \,\&\, Pr_l(\phi)<0$: $\Gamma_{P,\phi} = (\mu_t/\sigma_{t,\phi} + D_{l,\sigma})$

(iv) if $Pr_t(\phi)<0 \,\&\, Pr_l(\phi)>0$: $\Gamma_{P,\phi} = (D_{t,\phi} + D_{l,\phi})$ (22)

3. Linearization of Source Term

When the source term S depends on ϕ, the dependence can be linearized by Eq.(23). This is done because our nominally linear framework would allow only a formally linear dependence, and the incroporation of linear dependence is better than treating S as a constant.

$$S = S_C + S_P \phi_P \quad (23)$$

S_C includes in b, and $-S_P$ in a_P in Eq.(20).

4. Simple-like Algorithm

The solution algorithm is a matching one, that sweeps the domain in a slab-by-slab fashion. A slab is an X-Y plane of cells, and contains NX×NY cells. The code has three levels of iteration. The iteration level 1 in Fig. 2 the NX×NY system of equations for a variable ϕ at each slab, using either a generalized 2D version of the well-known Tri-Diagonal Matrix Algorithm(TDMA) or a Jacobi point by point procedure. The iteration level 2 has to blend together the changes effected for each variable separately. The pressure/velocity linkage has also to be dealt with this level. The pressure field has to be such that the velocities resulting from the momentum equations verify the continuity equation.

The iteration level 3 repeatedly solve the equations for all variables including pressure correction updating the corrections between them. In the slab by slab procedure, the off-slab values are assumed known, whereas they are not. As a consequence, the solution for the current slab is not the final one, and the solution procedure has to sweep all the slab in the domain several level. A datailed explanation on simple algorithm can be found in Patankar(1980).

5. Boundary Conditions

At wall U, V are zero and at the slot inlet a unform profile exist with U_{in} constant. $V_{in}=0$,

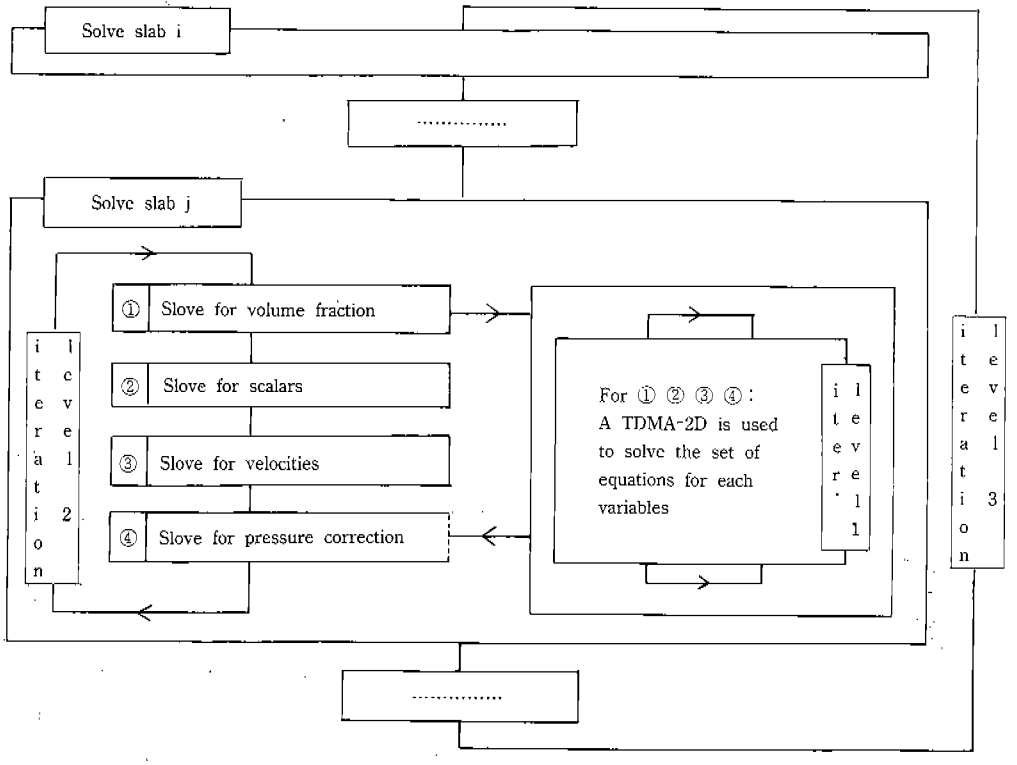

Fig. 2. Solution algorithm for two dimensional discretized equations

$k_{in}=i\ U_{in}^2$, and $\varepsilon^{3/2}/\alpha B_{in}$ where subscript 'in' denotes inlet. B is the width of the inlet, i is the turbulence intensity factor, and α is a turbulence intensity factor from 0.03 to 0.04 is recommended for pipe flow ; a value of 0.04 was used for this study. The turbulence intensity factor depends on velocity gradient, not on the specific flow geometry. The treatment for the wall region can be referred to Choi et al.(1990).

V. Results and Discussion

Air flow patterns in Fig. 4(a) and Fig. 5(a), revealed by liquid film bubbles in the flow (Randall & Battams, 1976) were used to explore the ability of the model and solution procedure to predict realistic air flow.

1. Experimental Procedure

The full-scale section of a livestock building used in this study has been described in detail in Carpenter et al. (1972) and Randall & Battams (1976). The section was 7.35m wide representing a typical span which may accommodate two pig pens and three passages. It was arranged with solid walls, 1.05m high, to form a feeding passage at each side and with a central wall to form two pens. The section of the experimented livestock building is shown in Fig. 4(a) without purlin, and Fig. 5(a) with purlin beneath ceiling. The depth of the section represented the length of one pen and the height was 2.14m to the eaves and 2.74m to the ridge. An insulated shell connected to an air conditioner and enclosing the side wall and roof allowed the temperature outside the section to be controlled at about 19℃. Ventilating air was exhausted from the shell by a propellar fan and the temperature inside the section varied according to the fan speed selected. Heat released from the stock was represented by 28 simulated pigs resulting, for some of the lower fan speeds, in a higher temperature in the section than would be experienced in practice. A purlin was attached to ceiling midway between the eaves and the ridge. The effects of purlin extending 300mm beneath the smooth ceiling were studied. It was 51mm thick and extended over the full length of the building section and were mounted at right angle to the ceiling.

Using liquid film bubbles illuminated by a narrow beam of light, photographs were taken through a transparent wall of the building, and sketches were made of the airflow patterns with particular regard to the deflections caused by the purlins.

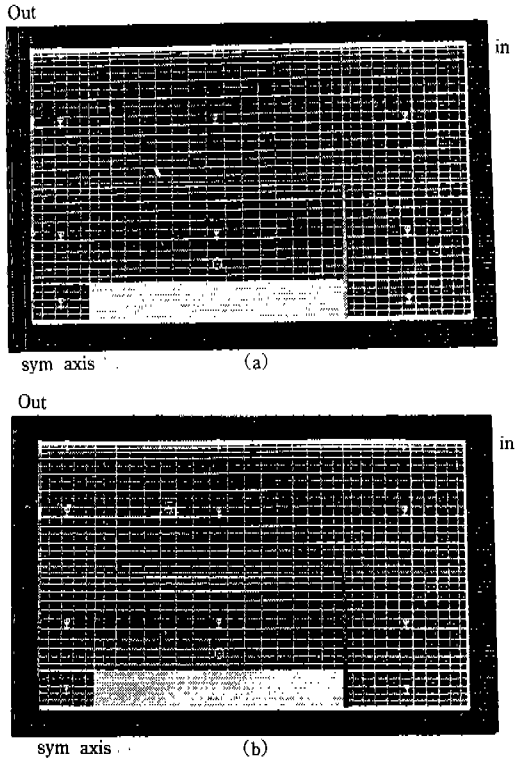

Fig. 3. Calculation domain griding non-uniformly for (a) without purlin (b) with purlin

The air jet, on entering the enclosure from the eaves through a slot 41mm wide and extending for the full length of the section tended to follow the slope of the ceiling. Fig. 3 shows the geometric sections of a livestock building for the study. The only difference of geometric configuration between the simulated structure and the prototype structure is the slope of roof. The horizontal roof was adapted in this study for calculation simplicity and for judicious guessing of lesser discrepancy from the actual flow motion.

2. Air Flow Pattern

1) Air flow pattern without purlin

Air flow patterns of the calculted in Fig. 4(b) and the observed in Fig. 4(a) are basically same regardless of the different roof arrangement. The calculated air distribution Fig. 4(b) shows primary recirculation in the region between the symmetric axis and internal solid wall(which separates the passage and the pig pen) and seconday recirculation between the internal solid wall and the inlet wall. The observed air distriburtion Fig. 4(a) only shows primary recirculation at the same region with the calculated.

The problem of the ventilation system is short-circuiting phenomenon of the air flow shown in Fig. 4(b). Most of the the entering air flow through the slot inlet at eave is exhausted by the fan at the ridge. A recirculating air forms the primary flow with lower velocity, so lower momentum rotates counterclockwise, and it again separates at the top of the internal solid wall. Some of them is entrained by the inlet air jet due to Coanda effect and the rest forms the secondary eddy rotating clockwise in the region between the internal solid wall and the inlet wall. Basically, air flow with less momentum has less capacity of diluting contaminated indoor air. Excessive harmful gases

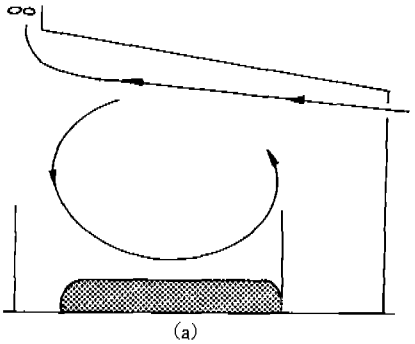

(a)

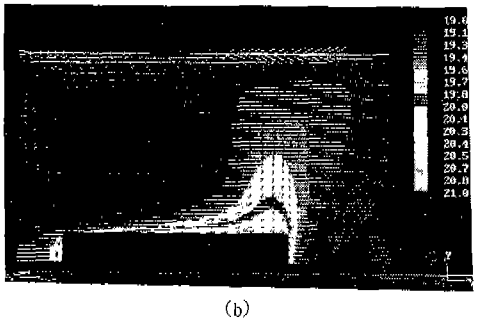

(b)

Fig. 4. a) the observed by randall & battams (1976) b) the calculated flow patterns

of dust may accumulate on the pigs or on the passage since the overall velocity is much smaller in the flow field so that it may not have enough kinetic energy to carry the contaminants out.

The internal solid wall separating the pen and the passage plays a significant role for modifying air flow as shown in Fig. 4(b). The obstruction leads to redirect air flow as well as to lower the kinetic energy of the flow due to the friction and impingement. Such a ventilation system should be modified for better mixing by lessening obstruction if possible or by replacing the solid to porous wall.

The observed air distribution of flow in Fig. 4(a) also shows the short-circuiting pheonomenon and a primary recirculation as same of Fig. 4(b). However, the observed can not show as much de-

tails as the simulated one. For example, the existence of the secondary flow might not be detected by the photograph due to smaller velocities in Fig. 4(a), It seems desirable to obtain much information through simulation rather than experiments.

2) Air flow pattern with purlin

Fig. 5(a) shows clearly the significant effect of obstruction located in the route of the inlet air jet flow. Purlin beneath the ceiling deflects the direction of the air flow and dissipate the kinetic energy of the flow by impingement. As shown in Fig. 5(a), two distinct recirculations can be observed ; one intermediate eddy is formed in behined of the purlin, which is not desirable and a primary recirculation in the middle of the whole flow field. A primary recirculation becomes smaller as compared to Fig. 4. However, Fig. 5(b) shows completely different air flow pattern with Fig. 5(a). The

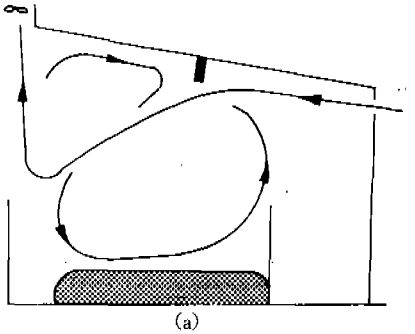

(a)

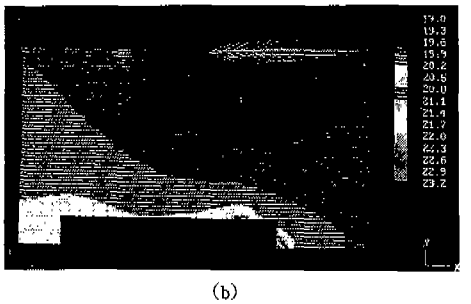

(b)

Fig. 5. a) the observation by randall & battams (1976) b) the calculated flow patterns

air jet in Fig. 5(b) impinging against the purlin extending 300mm perpendicularly to the ceiling dissipates most of its kinetic energy. Small eddies are observed in the front and behind region of the purlin. Most of air with lower velocity is exhausted to the outlet except an intermediate eddy in the upper right region of the whole flow field.

The deviation of the air distribution in Fig. 5(b) and Fig. 5(a), seems basically due to the geometrical difference of the roof. Although the detailed air distribution is not shown in Fig. 5(a), it is not difficult to figure out the air distribution in whole flow field. The air jet enters horizontally at eave in the inlet wall and it deflects to the inclined roof due to Coanda effect. Initially the entering air jet was a free jet, but it became a reattached wall jet due to Coanda effect. Substantial kinetic energy dissipates at the reattached point due to samll but strong eddy. The reattached air jet flow grows faster than initial wall jet so that some of jet flow may be beyond the reach of the purlin. The flow may form a primary recirculation. While initiall wall jet with higher kinetic energy for the geometry of Fig. 5(b)(refer to Fig. 3(b)) dissipates most of its energy at the purlin due to impingement so that it may not have enough momentum to overcome the negative pressure of the outlet.

Suppose the flow field in Fig. 5(b) is a right one, the whole field can be considered to be stagnant. The ventilation system of Fig. 5(b) can not dilute contaminants in the building. The information provided from the simulation analysis shown in Fig. 5(b) can be feedbacked for design purpose.

2. Temperature distribution

The entering air temperature was maintained 19℃ and the surface temperature of the simulated

pig was 38℃. Such a temperature difference between the air jet and the simulated pigs, creating buoyancy force, involves in the V-momentum equation(5). As shown in Fig. 4(b), low temperature is distributed in the primary reciculation region and higer temperaure distributed in the region between the solid wall and the upper surface of the simulated pigs. Fig. 5(a) confirms the fact that air flow redistributed scalars in the enclosure since the temperature distribution depends upon the route of air flow. Fig. 5(b) shows temperature stratification in the enclosure. Lower temperature is distributed in the upper region and higher in the lower due to incomplete mixing. This says that the ventilation system does not play its role.

VI. Conclusion

The TEACH-like program, which uses the standard k-ε turbulence model, was applied to a ventilated air space having obstruction ; the simulated pigs with heat flux, the internal solid walls and a purlin. Results were compared to experimental data and the following conclusions were drawn.

1. It is possible to predict, with reasonable accuarcy, overall flow patterns of air and temperature distribution in a ventilated space, represneting simple livestock buildings having obstructions, by solving discretized conservation equations and using the standard k-ε model.

2. Obstruction in a ventilated space,like the internal solid walls, the simulated pigs. and the purlin attached beneath the ceiling modifies air flow and/or creates dead regions. The obstacle like the purlin in the geometric configuration of Fig. 5 dissipates most kinetic energy of the air jet, which lead to imcomplete mixing due to lack of momentum. The obstruction in the route of the inlet air jet flow should be avoided since the inlet jet goverms whole flow field.

3. The venitlation system, having inlet at the eave and outlet at ridge leads air flow short-circuited. Such system reduces the effectiveness of the ventilation and creates the dead regions.

4. The buoyancy force originated from the temperature difference between the entering air and the body temperature of the simulated pigs moves air flow upwards. Heat accumulation can be observed in the stagnant region created by obstructions.

5. It is prerequisite to simulate air flow and temperature distributions in a ventilated space for design purpose to evaluate the efficiency of the ventilation system to be condstructed.

〈Symbols〉

- $a's$: coefficents in finite-domain equation in Eq. (20)
- b : source term of ϕ in Eq.(21)
- U : instantaneous velocity in Eq.(7)
- $\overline{U}_i$: mean velocity in Eq.(7)
- u_i : fluctuating velocity in Eq.(7)
- U : horizontal mean velocity
- V : vertical mean velocity
- k : turbulent kinetic energy
- ε : the rate of dissipation of turbulent kinetic energy
- h : enthalpy
- S_s : a source term in Eq.(19)
- ρ : density
- α : upwinding-scheme control parameter
- β : coefficient of gas expansion
- Γ_s : an exchange coefficient in Eq.(19)
- δ_{ij} : Cronical delta
- $C\mu$: coefficient
- μ_{eff} : effective tubvulent viscosity
- μ : laminar viscosity

μ_t : turbulent viscosity
σ : laminar Prandtl(Pr) number
σ_t : turbulent Prandtl number
ϕ : variable in question in Eq.(20)
Φ : instantaneous scalar quantity in Eq.(7)
$\overline{\Phi}_t$: mean scalar quantity in Eq.(7)
ϕ : fluctuating scalar quatity in Eq.(7)

〈**Subscrips**〉

p : grid node location at the center of the domain of pressure
N : grid node at north
S : grid node at south
E : grid node at east
W : gird node at west
T : time step node
D : diffusion
l : laminar
t : turbulent

Reference

1. Hellickson M. A. and J. N. Walker(editors). Ventilation of Agriculatural Structures. ASAE Monograph No. 6. St. Joseph. MI, 1983.
2. Hong Lim Choi. Ventilation of Agricultural Structures. Daegwang Pub, 1989.
3. Hong Lim Choi & Won Myung, Suh. Determination of Environmental Parameters for Agricultural Production Structures. J. Inst. Agr. Res. Util. Gyeongsang Nat'l University 22(2) : 221, 1988.
4. Barber E. M. Scale-Model Study of Incomplete Mixing in a Ventilated Air Space. Unpublished Ph. D. Thesis, University of Guelph, 1981.
5. Hong Lim Choi, Hyeon Tae Kim & Woo Joong Kim. Development of New Conceptual Ventilation Graphs for Mechanically Ventilated Livestok Buildings. J. of KSAE 33(3) : 91~100, 1991.
6. Albright L. D. Building Environmental Control, AE682 Lecture Notebook, Conrell Univesity, Ithaca, NY, 1984.
7. ASHRAE. Fundamentals. Am. Soc. Heating, Refri., Ari-Cond. Engrs. 1989.
8. Hong Lim Choi, L. D. Albright, M. B. Timmons & Z. Warhaft. An Application of the k-ε Turbulence Model to Predict Air Distribution in a Slot-Ventilated Enclosure. Transaction. ASAE 31(6) : 1804~1814, 1988.
9. Hong Lim Choi, L. D. Albright & M. B. Timmons. An Application of the k-ε Turbulence Model to Predict How a Rectangular Obstacle in a Slot-Ventilated Enclosure Affects Air Flow. Transaction. ASAE 33(1) : 274~281, 1990.
10. Fairbanks, F. L. Air Movement Studies in Dairy Stable Ventilation. Agric. Engr. 8(2) : 34, 1927.
11. Fairbanks, F. L. The Ventilation of Animal Shelters. Agric. Engr. 13(2) : 321~323, 19 32.
12. Pattie, D. R. & W. R. Milne. Ventilation Air Flow Patterns by Using of Models. Transation. ASAE 9(5) : 645~649, 1966.
13. Timmons, M. B. Internal Air Velocity as Affected by the Size and Location of Continuous Inlet Slots. Transaction. ASAE 27(5) : 1514~1517, 1984.
14. Tennekes, H. and J. L. Lumley, A First Course in Turbulence. MIT Press, Cambridge, MA, 1972.
15. Turbull, J. E. & J. A. Coates. Temperature and Air-Flow Patterns in a Controlled-Environment, Cage Poultry Building. Transaction. ASAE 14(1) : 109~113, 120, 1971.

16. Carpenter, G. A.,L. J. Mousley & J. M. Randall. Ventilation Investigation Using a Section of a Livestock Building and Air Flow Visualization by Bubbles. JAER 17(4) : 323~331, 1972.
17. Randall, J. M. The Prediction of Air flow Patterns in a Livestock Building. JAER 20(2) : 199~215, 1975.
18. Boon, C. R. Airflow Patterns and Temperture Distribution in an Expermental Piggery. JAER 23(2) : 129~139, 1978.
18. Patankar, P. V. Numerical Heat Transfer and Fluid Flow. McGraw-Hill Book Company. NY, 1980.
19. Timmons, M. B. Experimental and Numerical Study of Air Movement in Slot-Ventilated Enclosures. Unpublished Ph. D. Thesis, Cornell University, 1979.
20. Rodi, W. Turbulence Models and Their Applications in Hydraulics-A State of the Art Review.(1st ed). International Assocation for Hydraulic Research, Delft, 1984
21. Randall, J. M. & V. A. Battams. The Observed Influence of Surface Obstructions on the Airflow Pattern Within Livestock Building. JAER 21(1) : 33~39, 1976.